

Title:

Mixed Bernstein-Bézier Construction from Unstructured Mesh for Higher-order Finite Element Analysis of Plates and Shells

Authors:

Xiaoxiao Du, duxiaoxiao@buaa.edu.cn, Beihang University

Wei Wang, jrrt@buaa.edu.cn, Beihang University

Gang Zhao, zhaog@buaa.edu.cn, Beihang University

Keywords:

Mixed Bernstein-Bézier Polynomials, Isogeometric Analysis, Unstructured Mesh, *hp*-refinements, Plates and Shells

DOI: 10.14733/cadconfP.2019.186-191

Introduction:

Bernstein polynomials [4, 6] provide a series of attractive properties and elegant algorithms, e.g. de-Casteljau algorithm for various computational applications besides its widespread use in fields of CAGD and computer graphics. Nevertheless, they have received virtually no attention in finite element approximation for many decades since that the interpolated nodes might be expected in finite element method instead of the control points away from physical elements [1, 7]. In the traditional finite element method, CAD geometries should be approximately divided into mesh elements for analysis, which can consume up to 80% time of the whole process [8]. The gap between CAD and FEA will be bridged with the advent of isogeometric analysis (IGA) [3, 8] which directly employs the spline basis functions and control points of CAD geometries as the shape functions and nodes in FEA. This makes it possible to introduce Bernstein polynomials to FEA to better enjoy the elegant properties and algorithms of the Bernstein polynomials.

Motivated by the scenario of isogeometric analysis and some elegant properties and algorithms of Bernstein polynomials, this paper, from a geometric view, investigated the application of mixed Bernstein basis functions based higher-order finite element method to the analysis and simulation of plate and shell structures represented by unstructured triangular and quadrilateral mesh. Triangular Bernstein-Bézier patches and tensor-product Bézier patches are constructed in a simple and intuitive way over triangular and quadrilateral elements, respectively. The *h*- and *p*-refinements can be easily implemented on the constructed mixed Bernstein-Bézier patches. Reissner-Mindlin theory is employed to deduce the governing equations and stiffness matrices of plates and shells. Several numerical examples including classical benchmark problems and engineering applications are studied to validate the accuracy, robustness, and convergence of the presented Bernstein-Bézier finite element method.

Bézier Patches Construction:

Triangular and quadrilateral elements are the frequently-used and important elements for the analysis of surface geometries in the finite element method. Tensor-product Bézier surfaces over quadrilateral elements and triangular Bézier surfaces over triangular elements are firstly built by following two steps. The first step is to construct edge Bézier control points on each edge in the mesh model and the next is to build inner control points for each element according to the obtained boundary Bézier control points. In this section, bi-cubic tensor-product Bézier patches and cubic triangular Bézier patches are built over mesh elements.

Edge Control Points Construction:

For 2D plane mesh models, edges are divided into two parts: boundary edges and inner edges. We construct the Bézier control points for mesh boundary edges with a fairing strategy and for inner edges with a shape-preserving strategy. Tangent vectors of the boundary vertices are defined firstly. Assuming that v_1, v_2, v_3 are three successive boundary vertices as depicted in Fig. 1(a), tangent vector t_2 of the vertex v_2 are defined by the circumcircle of vertices v_1, v_2, v_3 with $Ov_2 \cdot t_2 = 0$ where point O is the center of the circumcircle. Tangent vector attached to each boundary vertex can be defined after iterating through all boundary vertices.

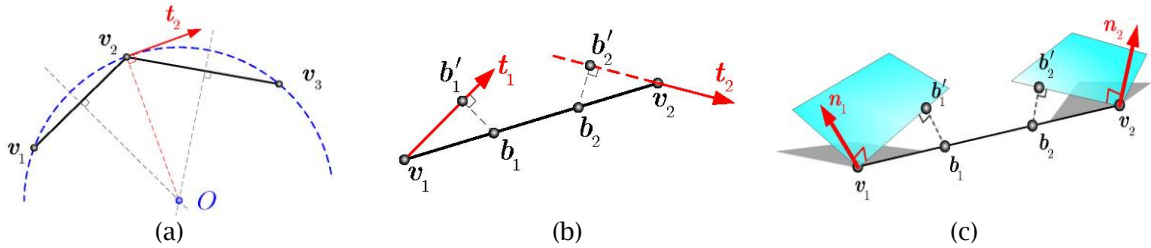


Fig. 1: Bézier Edge control points construction. (a)-(b) The tangent vector calculation and control points construction for plane mesh boundary edges, (c) Bézier control points construction for 3D surface Mesh edges.

With a tangent vector of each boundary vertex, we can choose suitable points as Bézier control points for each boundary edge. As shown in Fig. 1(b), e_{12} is a boundary edge and t_1, t_2 are two tangent vectors for vertices v_1 and v_2 , where e_{ij} denote the edge built with the vertices v_i and v_j . b_1, b_2 are two trisection points of the edge e_{12} with $b_1 = 2/3v_1 + 1/3v_2$, $b_2 = 1/3v_1 + 2/3v_2$. Bézier control points b'_1 and b'_2 are defined by the projection of two vertices b_1, b_2 onto the tangent vectors t_1, t_2 . In formulae for implementation, control points b'_1, b'_2 are given by:

$$b'_1 = v_1 + \frac{1}{3}[(v_2 - v_1) \cdot t_1] \cdot t_1, \quad b'_2 = v_2 + \frac{1}{3}[(v_1 - v_2) \cdot t_2] \cdot t_2. \quad (2.1)$$

The points v_1, b'_1, b'_2, v_2 are chosen as control points for each boundary edge and v_1, b_1, b_2, v_2 for each inner edge. For 3D surface mesh models, vertices and its normals are employed to construct edges control points as proposed in [10]. As demonstrated in Fig. 1(c), e_{12} is an arbitrary edge and n_1, n_2 denote the normals for the vertices v_1, v_2 . Control points b'_1, b'_2 are defined by the projection of trisection points b_1, b_2 of the edge e_{12} onto the corresponding normal plane and can be formalized as:

$$b'_1 = \frac{1}{3} 2v_1 + v_2 - [(v_2 - v_1) \cdot n_1] \cdot n_1, \quad b'_2 = \frac{1}{3} v_1 + 2v_2 - [(v_1 - v_2) \cdot n_2] \cdot n_2. \quad (2.2)$$

The Bézier control points for each mesh edge are obtained after the implementation of Eqns. (2.1)-(2.2). For arbitrary triangular or quadrilateral elements, we can find their all edge Bézier control points which are regarded as the boundary control points of triangular Bézier patch or tensor-product Bézier patch. Next the inner control points of different Bézier patches could be constructed based on the known boundary control points.

Triangular Bézier Inner Control Points Construction:

While three boundary control polygons of a triangular Bézier patch are given, the inner control points can be constructed by utilizing a mask given in [5]. This kind of triangular Bézier patches is also called

triangular permanence patches [5]. The inner control point \mathbf{b}_{111} of a cubic triangular Bézier patch could be defined by:

$$\mathbf{b}_{111} = \alpha(\mathbf{b}_{300} + \mathbf{b}_{030} + \mathbf{b}_{003}) + \beta(\mathbf{b}_{210} + \mathbf{b}_{120} + \mathbf{b}_{021} + \mathbf{b}_{012} + \mathbf{b}_{102} + \mathbf{b}_{201}). \quad (2.3)$$

A quadratic precision property could be obtained by choosing $\alpha = -1/6$ [5]. Then the above equation is rewritten as:

$$\mathbf{b}_{111} = E + (E - V)/2, \quad V = \frac{1}{3}(\mathbf{b}_{300} + \mathbf{b}_{030} + \mathbf{b}_{003}), \quad E = \frac{1}{6}(\mathbf{b}_{210} + \mathbf{b}_{120} + \mathbf{b}_{021} + \mathbf{b}_{012} + \mathbf{b}_{102} + \mathbf{b}_{201}), \quad (2.4)$$

which is equal to that from [10]. Therefore, the cubic triangular Bézier patch built with $\alpha = -1/6$ is a curved PN triangle. $\alpha = -1/6$ is also used in this paper.

Tensor-product Bézier Inner Control Points Construction:

Tensor-product Bézier patches are established over quadrilateral elements. Given boundary control points of a tensor-product Bézier patch, the inner control points could be generated by introducing a discrete Coons method presented in [5], which was also employed as the first step to build good parametrization of a computational domain for isogeometric analysis [11].

Given four boundary control points $\mathbf{b}_{0j}, \mathbf{b}_{nj}, \mathbf{b}_{i0}, \mathbf{b}_{im}, i = 0, 1, \dots, n, j = 0, 1, \dots, m$, the interior control points $\mathbf{b}_{ij}, 0 < i < n, 0 < j < m$ are defined by the discrete Coons method as:

$$\mathbf{b}_{ij} = \left(1 - \frac{i}{n}\right)\mathbf{b}_{0j} + \frac{i}{n}\mathbf{b}_{nj} + \left(1 - \frac{j}{m}\right)\mathbf{b}_{i0} + \frac{j}{m}\mathbf{b}_{im} - \left[1 - \frac{i}{n} \quad \frac{i}{n}\right] \begin{bmatrix} \mathbf{b}_{00} & \mathbf{b}_{0m} \\ \mathbf{b}_{n0} & \mathbf{b}_{nm} \end{bmatrix} \begin{bmatrix} 1 - j/m \\ j/m \end{bmatrix} \quad (2.5)$$

There also exists a mask to construct permanence patches [5]. The discrete Coons method is used to generate inner control points of a tensor-product Bézier patch in this work. Figures 2(a) and 2(d) illustrate a rotated letter 'g' plane mesh model and a car body 3D surface mesh model, both of which are constituted with few triangular elements and a bunch of quadrilateral elements. The mixed Bézier models are constructed from the unstructured meshes as shown in Figs. 2(b) and 2(e). Figures 2(c) and 2(f) present the distributions of the constructed Bernstein-Bézier mesh. Yellow and cyan elements represent triangular and rectangular Bézier elements, respectively. Red and blue solid dots (spheres) represent boundary control points and inner control points, respectively. It's easy to observe the mixed Bézier models are much smooth and real compared with the corresponding mesh models.

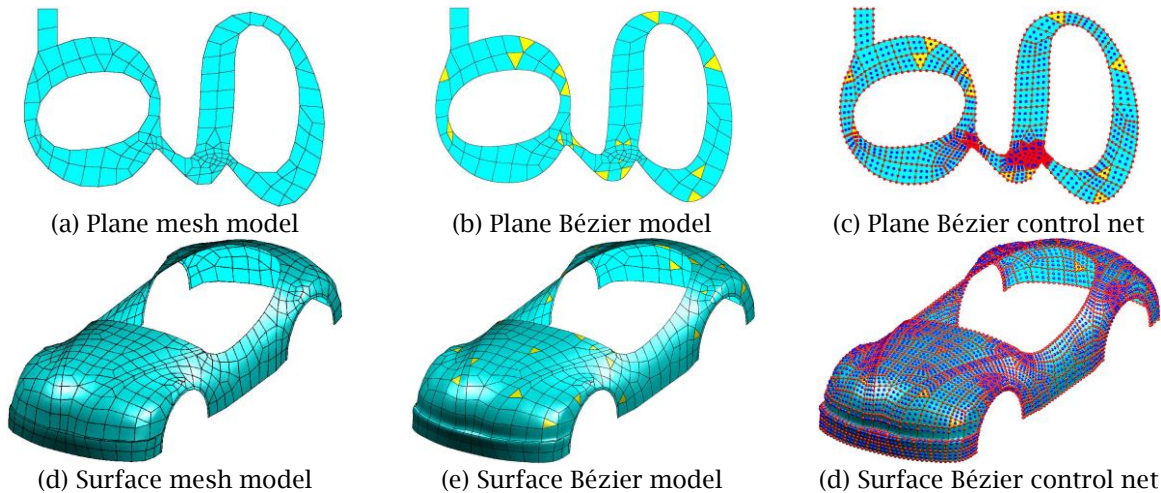


Fig. 2: Mixed Bézier reconstruction from a rotated letter 'g' plane model and car body surface model

Formulations:

Considering the static bending and free vibration of the Reissner-Mindlin plate, the variational form of the equilibrium equation in the context of elastodynamics can be written as:

$$\int_{\Omega} \delta \varepsilon_p^T \sigma_p d\Omega + \int_{\Omega} \delta u^T \rho \ddot{u} d\Omega = \int_{\Omega} \delta u^T \bar{b} d\Omega - \int_{\Gamma} \delta u^T \bar{t} d\Omega \quad (3.1)$$

where \bar{b} , \bar{t} and ρ denote the body force, traction force and density. The discretized governing equations derived for static bending problems are given as

$$\mathbf{K}u = F. \quad (3.2)$$

And for free vibration problems are given as

$$M\ddot{u} + \mathbf{K}u = 0. \quad (3.3)$$

where

$$\mathbf{K} = \int_{\Omega} \mathbf{B}^T \mathbf{D} \mathbf{B} d\Omega, \quad \mathbf{M} = \int_{\Omega} \mathbf{R}^T \mathbf{m} \mathbf{R} d\Omega. \quad (3.4)$$

To calculate the integration over elements, Gauss-Legendre quadrature rule is used for tensor-product Bézier patches and a collapsed Gaussian quadrature rule is used for triangular Bézier patches by collapsing the square to a triangle [9].

Numerical Examples:

Clamped Square Plate Under a Transverse Load:

In the plate bending problem, a unit square plate $[0, 1]^2$ with all sides fully clamped is investigated as shown in Fig. 3. Young's modulus $E = 10.92 \times 10^6$, Poisson ratio $\nu = 0.3$. The thickness-span ratio of the plate is 0.1. The square plate is built with 30 bi-cubic rectangular Bézier elements and 4 cubic triangular Bézier elements. The deflection w , bending moment M_x and rotation θ_x are investigated and plotted as shown in Fig. 3(b)-3(d).

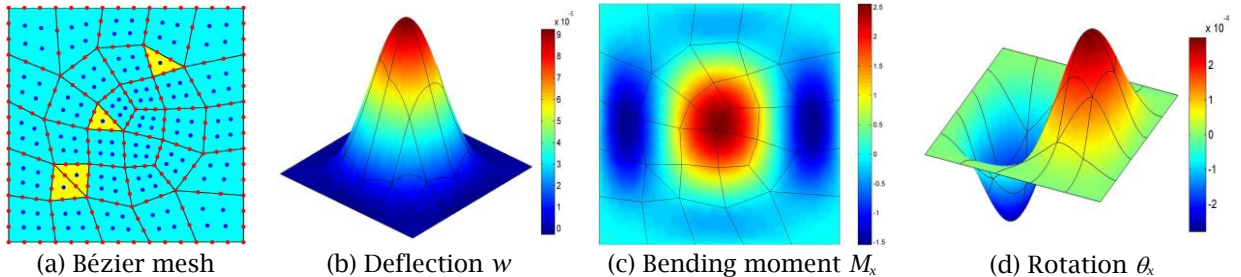


Fig. 3: Clamped unit square plate. (a) The constructed mixed Bézier mesh model and simulations results of (b) deflection w (c) bending moment M_x and (d) rotation θ_x .

Pinched Cylinder Subjected to a Concentrated Load:

Pinched cylinder from the so-called shell obstacle course [2] with rigid diaphragm ($u_x = u_z = \theta_y = 0$) is subjected to a pair of radial load P at the top and bottom middle position as shown in Fig. 4(a). Due to the symmetry property, only one eighth of the cylinder should be modeled and analyzed. Figure 4(b) shows the mixed Bézier mesh consisting of 9 triangular Bézier patches and 150 rectangular Bézier patches. The vertical displacement of the shell is presented in Fig. 4(c). The convergence of the vertical displacement at point C , against $\sqrt{\#elem}$ and $\sqrt{\#dof}$, is investigated among the mixed Bézier meshes, C^2 -continuity and C^0 -continuity NURBS mesh with different degrees as depicted in Fig. 5.

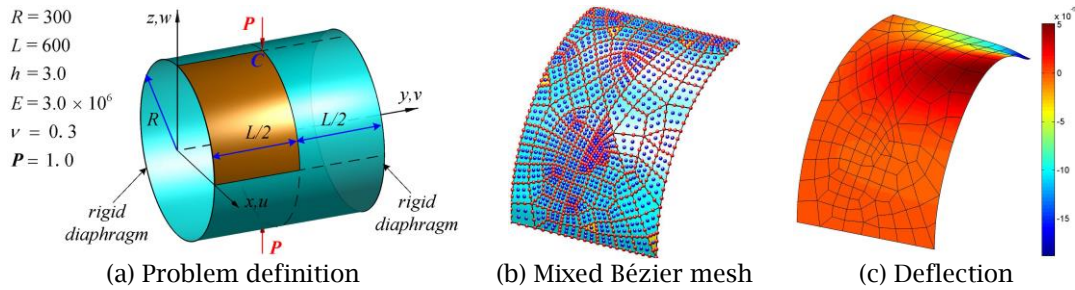


Fig. 4: Pinched cylinder. (a) The description and dimensions of the pinched cylinder, (b) the mixed Bézier mesh of one eighth of the pinched cylinder and (c) the vertical displacement.

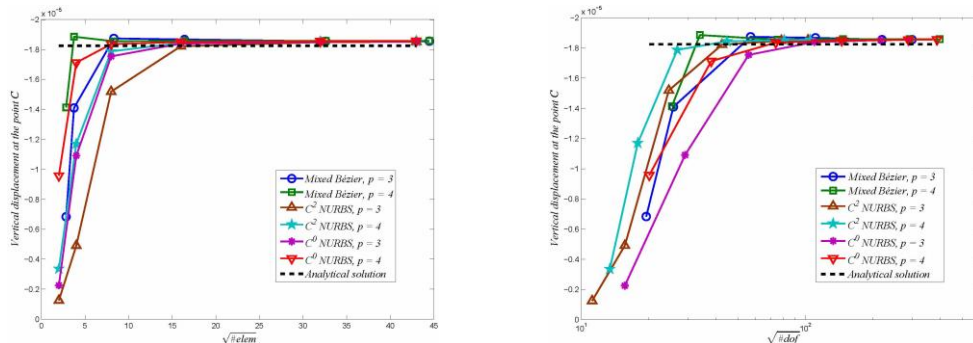


Fig. 5: Pinched cylinder: the convergence comparison of the vertical displacement at point *C* against the square root of the number of elements (Left) and the square root of the number of DOFs (Right).

Conclusions:

A novel method has been proposed to realize higher-order finite element analysis on unstructured mesh surface by the construction of triangular Bézier patches over triangular elements and tensor-product Bézier patches over quadrilateral elements. The procedures of construction are simple and intuitive. The numerical results show that this method is feasible for its near equivalent accuracy and convergence with isogeometric analysis so it provides an alternative for engineering scenarios when higher-order finite elements are required. Also for incomplete mesh models that are often too coarse to give a fair result but need to be further refined, this method can be especially helpful and give more accuracy compared with the resort to the classical finite element method.

Acknowledgement:

This work is financially supported by the Natural Science Foundation of China (Project Nos. 61572056).

References:

- [1] Ainsworth, M.; Andriamaro, G.; Davydov, O.: Bernstein-Bézier finite elements of arbitrary order and optimal assembly procedures, *SIAM Journal on Scientific Computing*, 33(6), 2011, 3087-3109. <https://doi.org/10.1137/11082539X>
- [2] Belytschko, T.; Stolarski, H.; Liu, W.K.; Carpenter, N.; Ong, J.S.: Stress projection for membrane and shear locking in shell finite elements, *Computer Methods in Applied Mechanics and Engineering*, 51(1-3), 1985, 221-258. [https://doi.org/10.1016/0045-7825\(85\)90035-0](https://doi.org/10.1016/0045-7825(85)90035-0)
- [3] Cottrell, J.A.; Hughes, T.J.; Bazilevs, Y.: *Isogeometric analysis: toward integration of CAD and FEA*, John Wiley & Sons, 2009.
- [4] Farin, G.: Triangular Bernstein-Bézier patches, *Computer Aided Geometric Design*, 3(2), 1986, 83-127. [https://doi.org/10.1016/0167-8396\(86\)90016-6](https://doi.org/10.1016/0167-8396(86)90016-6)
- [5] Farin, G.; Hansford, D.: Discrete coons patches, *Computer Aided Geometric Design*, 16(7), 1999, 691-700. [https://doi.org/10.1016/S0167-8396\(99\)00031-X](https://doi.org/10.1016/S0167-8396(99)00031-X)

- [6] Farin, G.E.; Farin, G.: Curves and surfaces for CAGD: a practical guide, Morgan Kaufmann, 2002.
- [7] Farouki, R.T.: The Bernstein polynomial basis: A centennial retrospective. *Computer Aided Geometric Design*, 29(6), 2012, 379-419. <https://doi.org/10.1016/j.cagd.2012.03.001>
- [8] Hughes, T.J.; Cottrell, J.A.; Bazilevs, Y.: Isogeometric analysis: CAD, finite elements, NURBS, exact geometry and mesh refinement, *Computer Methods in Applied Mechanics and Engineering*, 194(39-41),2005, 4135-4195. <https://doi.org/10.1016/j.cma.2004.10.008>
- [9] Lyness, J.N.; Cools, R.: A survey of numerical cubature over triangles, In *Proceedings of Symposia in Applied Mathematics*, 48, 1994, 127-150. <https://doi.org/10.1090/psapm/048/1314845>
- [10] Vlachos, A.; Peters, J.; Boyd, C.; Mitchell, J.L.: Curved PN triangles, In *Proceedings of the 2001 symposium on Interactive 3D graphics*, 2001, 159-166. <https://doi.org/10.1145/364338.364387>
- [11] Xu, G.; Murrain, B.; Duvigneau, R.; Galligo, A.: Parameterization of computational domain in isogeometric analysis: methods and comparison, *Computer Methods in Applied Mechanics and Engineering*, 200(23-24), 2011, 2021-2031. <https://doi.org/10.1016/j.cma.2011.03.005>